Comparative Analysis of System Performance Between F-SCAN and DBF SARs

Bo Li, *Member, IEEE*, Pingping Lu, *Senior Member, IEEE*, Zhang Yunjun, *Member, IEEE*, Yijiang Nan, and Tianyuan Yang

***Abstract*—Frequency scanning (F-SCAN) synthetic aperture radar (SAR) offers unique advantages over digital beamforming (DBF) SAR for high-performance imaging. However, F-SCAN SAR introduces several new pitfalls, such as reduced effective average power, potential increase in data rate, and performance constrained by available bandwidth, which require more rigorous mathematical analysis. In this letter, we first introduce four performance ratios derived mathematically to compare the system performance between the two imaging techniques and then propose an optimization strategy for design of system parameters. Our analysis shows that F-SCAN SAR should not be considered a superior alternative for DBF SAR, but rather an important complement, as the former may result in degraded performance in specific scenarios. With a large available bandwidth, F-SCAN SAR would be well-suited for applications requiring very wide swaths with medium- to low-range resolutions.**

***Index Terms*—Comparative analysis, digital beamforming (DBF), feasible region of system parameter, frequency scanning (F-SCAN), synthetic aperture radar (SAR), system performance.**

I. Introduction

FREQUENCY scanning (F-SCAN) synthetic aperture radar (SAR) [1], [2], [3], [4], [5], [6] and digital beamforming (DBF) SAR [7], [8] are two advanced imaging modes developed to address the dilemma in conventional SAR: achieving high antenna gain while maintaining a wide swath width. Both methods scan the swath using narrow beams, thereby decoupling antenna height from swath width and enhancing system performance in terms of noise-equivalent sigma zero (NESZ) and range-ambiguity-to-signal ratio (RASR). Several studies have focused on comparing the system performance of F-SCAN and DBF SARs. Guccione et al. [3] first conducted a preliminary system performance comparison (SPC), refining the definitions of NESZ and RASR. Younis et al. [4] extended this work by deriving dedicated operational parameters and providing deeper insights.

Compared to DBF SAR, F-SCAN SAR offers three distinct advantages: higher transmit gain, reduced system complexity, and a shorter echo window length (EWL) [1], [2], [3], [4], [5], [6]. At first glance, F-SCAN SAR may appear similar to DBF SAR and could initially be considered a superior alternative [1], [2], [3]. However, more thorough mathematical derivations are needed to better support this viewpoint, as F-SCAN SAR introduces several risks that constrain how system parameters are chosen. The aim of this letter is to mathematically analyze and clarify potential confusions arising from using a narrow and dynamic transmit beam. When comparing F-SCAN SAR with DBF SAR under the same total antenna height, swath width, and range resolution, three key aspects should be considered as follows.

1) *Point 1: Does F-SCAN SAR always outperform in RASR?*
2) *Point 2: Does F-SCAN SAR consistently achieve better SNR across the swath?*
3) *Point 3: Does F-SCAN SAR require a higher data rate?*

To answer these questions, we propose four system performance ratios to quantitatively compare the two imaging modes, then define a feasible region for system design, and propose an optimization strategy to guide the selection of system parameters for specific tasks.

II. Brief Review of F-SCAN Imaging

This section introduces the basic principles and key system parameters, providing the theoretical foundation for mathematical derivations in Sections III and IV.

A. Basic Operation Principle

The basic principle of F-SCAN SAR is to transmit a frequency-modulated signal using a frequency-dispersive antenna [4]. Then, a frequency-dependent beam is generated, which scans a wide swath from far to near range. The closed-form expression for scan angle θ (i.e., look angle) is given as follows:

$$\theta = \theta_c + \frac{\theta_{\text{sc}}}{B_F} \cdot f, \quad f \in \left[-\frac{B_F}{2}, \frac{B_F}{2}\right] \tag{1}$$

where $\theta_c = (\theta_f + \theta_n)/2$ is the center look angle of swath, and θ_f and θ_n denote the far- and near-range look angles, respectively. θ_{sc} represents the angular scan extent. The instantaneous frequency f can be normalized to $[-B_F/2, B_F/2]$, where B_F is the transmit bandwidth of SAR system. With a frequency-modulated signal, instantaneous variation in the transmitted signal's frequency can be mapped to a corresponding change in the scan angle over time. The link between the scan angle θ and time t is expressed as

$$\theta = \theta_c - \frac{\theta_{\text{sc}}}{T_F} \cdot t, \quad t \in \left[-\frac{T_F}{2}, \frac{T_F}{2}\right] \tag{2}$$

Received 27 June 2025; revised 28 September 2025; accepted 16 October 2025. Date of publication 20 October 2025; date of current version 30 October 2025. This work was supported by the National Science Fund for Excellent Young Scholars under Grant 62422121. *(Corresponding author: Pingping Lu.)*

The authors are with the National Key Laboratory of Microwave Imaging, Aerospace Information Research Institute, Chinese Academy of Sciences, Beijing 100190, China (e-mail: libo202@mails.ucas.ac.cn; lupp@aircas.ac.cn).

Digital Object Identifier 10.1109/LGRS.2025.3623992

where T_F is the transmit pulse duration. It is worth noting that an important property of the F-SCAN SAR is that the transmit bandwidth and pulse duration are "distributed" across the entire swath.

B. Several System Parameters

In F-SCAN SAR, dwell bandwidth represents the range of effective frequencies observed by a point target during the beam illumination period and can be derived as follows:

$$B_{Fd} = \alpha_b B_F \tag{3}$$

where $\alpha_b = \theta_{\text{el}}/\theta_{\text{sc}}$ denotes the dwell factor, and θ_{el} is the elevation beamwidth [4]. Similarly, the portion of the transmit pulse duration intercepted by a point target is called the dwell time, which is mathematically expressed as

$$\tau_F = \alpha_b T_F. \tag{4}$$

Another important system parameter for F-SCAN SAR is the operation point O_p, which is defined as

$$O_p = \frac{T_F}{T_0} = \frac{cT_F}{2W_r} \cdot \frac{\theta_{\text{sw}}}{\theta_{\text{sc}}}. \tag{5}$$

W_r is the slant range extent and $\theta_{\text{sw}} = \theta_{\text{sc}} - \theta_{\text{el}}$ is the angular swath extent. When the transmit pulse duration equals intrinsic pulse duration T_0, the near- and far-range echoes arrive simultaneously [4].

For the analysis that follows, we define the relative transmit antenna height (RTAH) as

$$h_{\text{RT}} = \frac{h_F}{h_D} = \frac{\theta_{\text{sw}}}{\theta_{\text{el}}} \tag{6}$$

where h_{RT} is defined as the F-SCAN SAR antenna height h_F normalized by the DBF SAR antenna height h_D, for imaging the same swath.

III. System Performance Ratios

The following system performance ratios are developed to investigate SPC with respect to RASR, NESZ, data rate, and RQF. To ensure a fair range-dimension comparison, the azimuth parameters of both systems are initially specified. The system PRF and antenna length are assumed to be feasible, satisfying swath width, azimuth resolution, and ambiguity constraints. To eliminate azimuth-related effects, identical azimuth-dimension parameters are assigned to both systems.

A representative X-band spaceborne SAR system is considered, with mission requirements drawn from authoritative design examples [1], [6]; the key parameters are listed in Table I. The pulse repetition frequency (PRF) is selected to satisfy swath width and azimuth resolution requirements. The antenna size is determined based on ambiguity performance, SNR, and other relevant factors. The DBF SAR transmit beamwidth is to be assumed adjustable via antenna tapering to maintain a constant swath. It should be noted that all subsequent definitions, derivations, and analyses are based on fundamental principles and are independent of specific system parameters. This exemplary system serves solely to illustrate and verify the comparative performance analysis.

TABLE I
System Parameters of Simulations [1], [6]

Parameter	F-SCAN SAR	DBF SAR
Orbit height	514 km	
Carrier frequency	9.80 GHz	
Look angle extent	18.45°-45.14°	
Swath wide/ Resolution	80 km / 1 m	
PRF	994 Hz-1209 Hz	
Number of digital Rx channel (el.x az.)	1 x 10	4 x 10
Antenna height (Tx/Rx)	1.4 m / 1.4 m	0.35m / 1.4 m
Antenna length (Tx/Rx)	1.5 m / 15 m	1.5 m / 15 m

A. RASR Ratio

It has been widely reported that F-SCAN SAR achieves superior RASR performance compared to DBF SAR [1], [2], [3], [4], [5], primarily due to its higher transmit antenna gain. However, a rigorous mathematical proof or detailed quantitative analysis to support this claim is still lacking. To this end, we define the RASR ratio between the two imaging modes as follows:

$$\beta_{\text{RASR}} = \frac{\text{RASR}_F}{\text{RASR}_D} = P_D^T(\theta - \theta_c) \cdot \frac{\sum_i \frac{P_F^T(\theta_i-\theta)P_F^R(\theta_i-\theta)}{R^3(\theta_i)\sin(\eta_i)}}{\sum_i \frac{P_D^T(\theta_i-\theta_c)P_D^R(\theta_i-\theta)}{R^3(\theta_i)\sin(\eta_i)}} \tag{7}$$

where θ_i and η_i denote the look angle and incidence angle for the ith range ambiguity signal, relative to the target signal at look angle θ. P denotes the normalized antenna pattern. The superscripts ^{T} and ^{R} indicate the transmit and receive antennas, while the subscripts $_D$ and $_F$ correspond to DBF SAR and F-SCAN SAR systems, respectively. F-SCAN SAR consistently provides higher signal power than DBF SAR, particularly at swath edges, with a typical gain of approximately 3 dB.

However, as illustrated in Fig. 1(a), the range ambiguity signals for edge targets lie closer to the antenna main lobe, which potentially result in increased ambiguity power at large incidence angles. This effect intensifies when h_{RT} approaches 1. Furthermore, RASR ratio satisfies the following inequality:

$$\beta_{\text{RASR}} \le P_D^T(\theta - \theta_c) \cdot \sum_i \frac{P_F^T(\theta_i - \theta)}{P_D^T(\theta_i - \theta_c)}. \tag{8}$$

The first term in (8) represents the ratio of signal power, which is always less than 1. The second term refers to the sum of individual ambiguity-signal-power ratios, which might exceed 1. Fig. 1(b)–(d) presents the RASR of both systems and the corresponding RASR ratios for different h_{RT}. Although F-SCAN SAR does not consistently outperform DBF SAR at all look angles, it achieves a better average RASR, particularly at large h_{RT}.

Thus, a possible conclusion is that F-SCAN SAR is expected to operate at a large h_{RT}, i.e., swath-to-beamwidth ratio $\theta_{\text{sw}}/\theta_{\text{el}} \gg 1$.

B. NESZ Ratio

Although the scanning-on-transmission mode of F-SCAN SAR allows for high transmit gain over the entire swath, the effective average power delivered to each target is reduced, since each target is illuminated only during the dwell time.

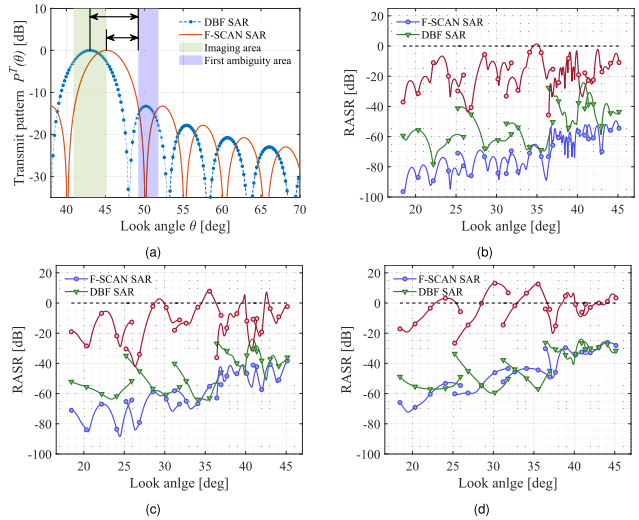

Fig. 1. (a) Spatial distribution of signal and ambiguity-signal power relative to transmit pattern with $h_{\mathrm{RT}} = 1$. RASR and corresponding RASR ratios with (b) $h_{\mathrm{RT}} = 4$, (c) $h_{\mathrm{RT}} = 2$, and (d) $h_{\mathrm{RT}} = 1$.

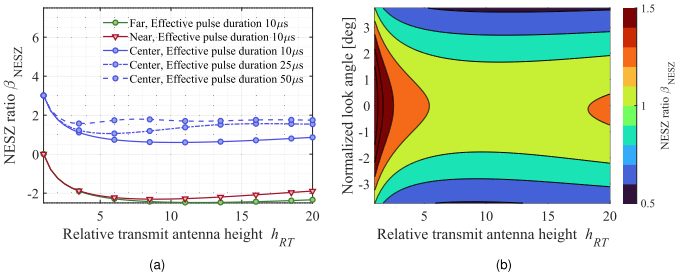

Fig. 2. (a) Variation of β_{NESZ} at the swath center and edges. (b) β_{NESZ} contour as a function of normalized look angle and h_{RT}.

Assuming that the effective average powers are identical in two systems, we define the NESZ ratio between the two imaging modes accordingly

$$\beta_{\mathrm{NESZ}} = \frac{\mathrm{NESZ}_F}{\mathrm{NESZ}_D} = R_{\mathrm{PEL}}(\theta) \cdot \frac{\theta_{\mathrm{sc}}}{N_e \theta_{\mathrm{el}}} \le R_{\mathrm{PEL}}(\theta) \cdot \left(1 + \frac{\theta_{\mathrm{el}}}{\theta_{\mathrm{sw}}}\right) \le 2 \tag{9}$$

with

$$R_{\mathrm{PEL}}(\theta) = \frac{\int_{\chi_\vartheta} P_D^T(\vartheta) P_D^R(\vartheta) d\vartheta}{\int_{\chi_\vartheta} P_F^T(\vartheta) P_F^R(\vartheta) d\vartheta}. \tag{10}$$

R_{PEL} is the two-way pulse-extent-loss (PEL) ratio within the angular pulse extent χ_ϑ [4], and depends on the effective pulse duration, look angle, and orbit height. N_e represents the number of digital channels in the DBF SAR system. Equation (9) is simple but essential for understanding. It is important to note that β_{NESZ} at the swath center exceeds 1, as shown in Fig. 2(a). This arises because F-SCAN SAR operates with a two-way narrow beam, yielding $R_{\mathrm{PEL}}(\theta_c) > 1$, while the transmit average power decreases by a factor of $\theta_{\mathrm{el}}/\theta_{\mathrm{sc}}$. NESZ is generally better at the swath edges, allowing F-SCAN SAR to operate with lower peak power while still satisfying NESZ requirements. Fig. 2(a) also shows the effect of effective pulse duration on β_{NESZ}, and Fig. 2(b) illustrates the NESZ ratio contour relative to RTAH, highlighting a potential risk associated with two-way PEL in F-SCAN SAR.

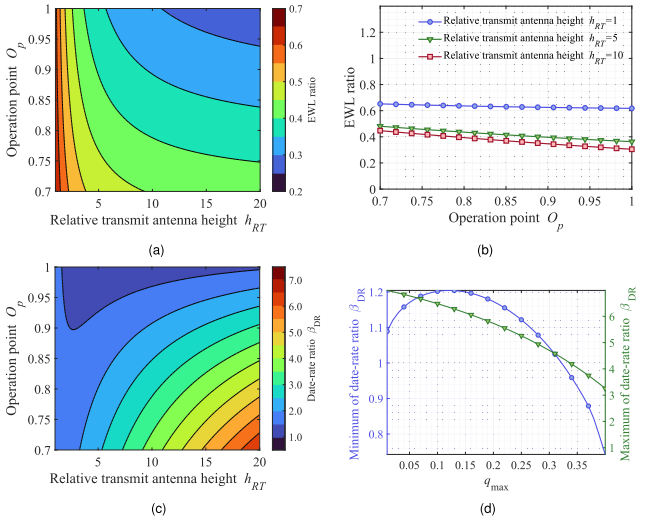

Fig. 3. (a) Contour plot of EWL ratio as a function of h_{RT} and O_p. (b) Variation of the EWL ratio with O_p for different h_{RT} values. (c) Contour plot of β_{DR} as a function of h_{RT} and O_p for $q_{\max} = 0.1$. (d) Boundary of β_{DR} as a function of $q_{\max}$.

Furthermore, since the beamwidth of DBF SAR is no less than θ_{sw}, the lower bound of the NESZ ratio can be derived as

$$\beta_{\mathrm{NESZ}} > \frac{1}{2} \cdot \left(1 + \frac{\theta_{\mathrm{el}}}{\theta_{\mathrm{sw}}}\right) > \frac{1}{2}. \tag{11}$$

The inequalities (9) and (11) show that the NESZ in F-SCAN SAR degrades by up to 3 dB relative to DBF SAR across the entire swath, while the maximum possible improvement remains below 3 dB.

Overall, the comparison of NESZ performance reveals that F-SCAN SAR benefits more from increased antenna height or a wider swath.

C. Data Rate Ratio

The data rate is a critical system parameter that reflects the satellite's requirements for on-board memory and downlink capacity. One notable advantage of F-SCAN SAR is its effective reduction of EWL while maintaining the swath width, which is given by

$$T_{Fe} = \left[1 - O_p\left(1 - \frac{\alpha_b}{1-\alpha_b}\right)\right] \frac{2W_r}{c} + T_{\mathrm{res}} \tag{12}$$

where T_{res} represents the residual time in F-SCAN SAR [4], [5]. This compressed EWL effectively reduces the data rate [3], [4], [5]. However, to achieve the same range resolution, F-SCAN SAR requires a transmit bandwidth several times greater than that of DBF SAR, leading to an increase in the data rate. This section examines whether F-SCAN SAR requires a higher data rate.

Assuming real-time DBF processing can be implemented onboard the DBF SAR system, the data rate ratio between the two imaging modes is defined as follows:

$$\beta_{\mathrm{DR}} = \frac{DR_F}{DR_D} = \frac{B_F}{B_D} \cdot \frac{T_{Fe}}{T_{De}} = \frac{1}{\alpha_b}\left\{\left[1 - O_p\left(1 - \frac{\alpha_b}{1-\alpha_b}\right)\right]\left(\frac{1-2q_{\max}}{1-q_{\max}}\right) + \frac{T_{\mathrm{res}}}{T_{De}}\right\} \tag{13}$$

where $q_{\max} = \tau_D/(\tau_D + T_{De})$ represents the maximum duty cycle of the DBF SAR, and τ_D and T_{De} denote the pulse duration and EWL in DBF SAR, respectively. The second term in (13) describes the EWL ratio between the two systems. Fig. 3(a) illustrates how the EWL compression ratio varies with h_{RT} (i.e., dwell factor α_b) and O_p. O_p is typically no greater than 1, as the flexibility of the available swath position decreases when $O_p > 1$. However, maintaining $O_p = 1$ is challenging, as larger values of O_p correspond to longer transmit pulse duration, which may be limited by the system's duty cycle. Fig. 3(b) depicts the variation of EWL ratio with O_p at different RTAHs. The results show that the degree of EWL compression decreases significantly, i.e., the EWL ratio increases when $h_{\mathrm{RT}} = 1$ (i.e., $\alpha_b = 0.5$), representing the most unfavorable condition for F-SCAN SAR.

The data rate ratio can be expressed as the product of the EWL ratio between the two systems, multiplied by $1/\alpha_b$. The effect of α_b on β_{DR} does not follow a simple monotonic function, as illustrated in Fig. 3(c). A smaller α_b (i.e., a larger RTAH) increases the data rate due to the larger transmit bandwidth but improves EWL compression, which reduces β_{DR}. It can be found from (13) that β_{DR} is also influenced by $q_{\max}$, which may cause the β_{DR} to exceed 1, even when an optimal RTAH and a large O_p are selected. Fig. 3(d) illustrates the boundary of β_{DR} as it varies with $q_{\max}$, assuming that $h_{\mathrm{RT}} \in [1, 20]$ and $O_p \in [0.7, 1]$.

In conclusion, F-SCAN SAR does not always require a higher data rate compared to DBF SAR, especially when optimal system parameters and relatively small swath are used.

D. RQF Ratio

We define the ratio of swath width to range resolution as the RQF. RQF characterizes the overall performance of system in achieving the optimal range resolution and maximum swath width subject to the constraints of PRF and available bandwidth. When two systems have the same swath width and range resolution, the RQF ratio equals 1 and can be expressed as

$$\beta_{\mathrm{RQF}} = \frac{Q_F}{Q_D} = \frac{B_{\mathrm{RT}}\theta_{\mathrm{el}}}{\theta_{\mathrm{el}} + \theta_{\mathrm{sw}}} \le \frac{B_{\mathrm{RT}}}{2}\sqrt{\frac{\theta_{\mathrm{el}}}{\theta_{\mathrm{sw}}}} \le \frac{B_{\mathrm{RT}}}{2} \tag{14}$$

where Q_F and Q_D denote the RQFs of F-SCAN SAR and DBF SAR, respectively. $B_{\mathrm{RT}} = B_F/B_D$ is the relative transmit bandwidth. In F-SCAN SAR, range resolution is inherently coupled with swath width, which limits Q_F and consequently imposes an upper bound on β_{RQF}. The underlying inequality (14) is that F-SCAN SAR would require a transmit bandwidth at least twice as large as DBF SAR to achieve an equal or larger RQF, as shown in Fig. 4(a). This requirement may exceed the available bandwidth, leading to potential insufficiency.

Therefore, the constraint imposed by the available bandwidth $B_{r,\max}$ should be taken into account when evaluating F-SCAN SAR's performance. For a specified range resolution ρ_r, the relative transmit bandwidth B_{RT} satisfies

$$B_{\mathrm{RT}} \le \frac{B_{r,\max}}{B_{r,D}} = \frac{2\rho_r B_{r,\max}}{c} \tag{15}$$

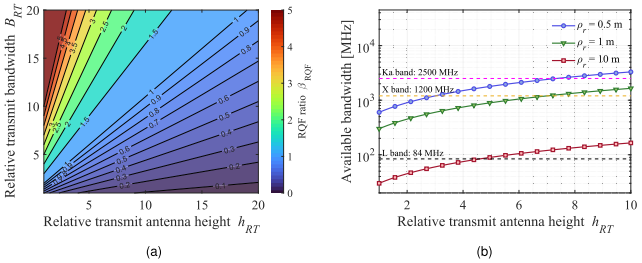

Fig. 4. (a) Contour plot of β_{RQF} as a function of h_{RT} and B_{RT}. (b) Required available bandwidth for F-SCAN SAR as a function of h_{RT} for different range resolutions.

where c is the speed of light. When both (14) and (15) hold, the available bandwidth is constrained by the following inequality:

$$B_{r,\max} \ge \frac{c\,(1 + h_{\mathrm{RT}})}{2\rho_r}. \tag{16}$$

As shown, $B_{r,\max}$ required for F-SCAN SAR has a lower bound determined by the desired range resolution and RTAH. Fig. 4(b) illustrates the required available bandwidth of F-SCAN SAR as a function of the RTAH for various range resolutions. Thus, achieving both high resolution and wide swath with F-SCAN SAR demands significantly greater bandwidth.

In summary, F-SCAN SAR is particularly suitable for systems operating at higher carrier frequencies, such as X-band, Ka-band, or even higher.

IV. Optimal Parameter Design for F-SCAN SAR

The coupling between available bandwidth and swath width results in a complex interplay among system performances in F-SCAN SAR, as discussed in Section III. Consequently, the optimal system parameter design is critical to achieve the desired performance.

A. Feasible Parameter Region

Given the swath width and spatial resolution, the key system parameters influencing performance are the transmit antenna height and pulse duration. These parameters can be mapped to the RTAH and the operation point. Following the principles in [9], these two variables define a 2-D rectangular plane, as illustrated in Fig. 5. This plane, referred to as the parameter region, can be expressed as

$$\begin{cases} l_{\mathrm{RT}} \le h_{\mathrm{RT}} \le u_{\mathrm{RT}} \\ l_p \le O_p \le u_p \end{cases} \tag{17}$$

where l and u denote the lower and upper bounds of the variable, respectively. Obviously, the parameter region provides the SAR system designer with considerable freedom in system parameter selection. Primary constraints on system performance can be represented by a feasible parameter region as follows:

$$\begin{cases} \beta_{\mathrm{RASR}_m}(h_{\mathrm{RT}}, O_p) \le u_{\mathrm{RASR}} \\ \beta_{\mathrm{NESZ}_c}(h_{\mathrm{RT}}, O_p) \le u_{\mathrm{NESZ}_c} \\ \beta_{\mathrm{NESZ}_f}(h_{\mathrm{RT}}, O_p) \le u_{\mathrm{NESZ}_f} \\ \beta_{\mathrm{DR}}(h_{\mathrm{RT}}, O_p) \le u_{\mathrm{DR}} \end{cases} \tag{18}$$

where β_{NESZ_c}, β_{NESZ_f}, and β_{RASR_m} represent the maximum NESZ loss of F-SCAN SAR at the swath center, NESZ

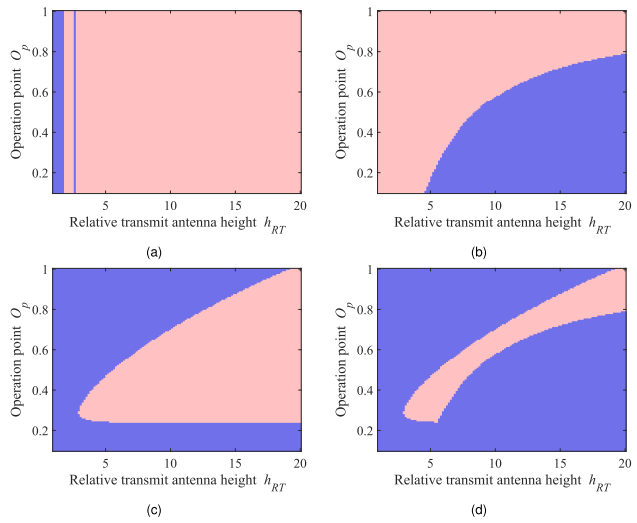

Fig. 5. Feasible parameter regions are marked in pink, and infeasible regions are marked in blue. Subfeasible parameter regions are defined by (a) $\beta_{\mathrm{RASR}_m} \leq 0.25$, (b) $\beta_{\mathrm{DR}} \leq 5$, and (c) both $\beta_{\mathrm{NESZ}_c} \leq 1.41$ and $\beta_{\mathrm{NESZ}_F} \leq 0.63$. (d) Full feasible parameter region is determined by the intersection of the three subfeasible regions.

improvement of F-SCAN SAR at the far-range, and mean RASR value, respectively. Clearly, the optimal feasible parameter region is the intersection of the subfeasible parameter regions derived from the system performance constraints, as shown in Fig. 5.

To investigate parameter tradeoffs in F-SCAN SAR design, we examine how the upper bounds in (18) influence the distribution and area of the feasible region. Reducing u_{RASR_m} contracts the subfeasible region in Fig. 5(a) along the large h_{RT} axis, whereas F-SCAN SAR maintains relatively good RASR performance even at small h_{RT}. Increasing u_{NESZ_f} and decreasing u_{NESZ_c} improve NESZ performance, but the subfeasible region in Fig. 5(c) contracts significantly along large h_{RT} and medium O_p, compressing the available parameter space and increasing the risk of an empty feasible region. Similarly, reducing u_{DRR} shrinks the subfeasible region in Fig. 5(b) along low h_{RT} and large O_p. In summary, designing h_{RT} requires considering: 1) not exceeding the maximum set by available bandwidth $B_{r,\max}$ and 2) prioritizing the tradeoff between NESZ and data rate. Designing O_p must account for system duty cycle to allow sufficient beam position selection [4] and balance data rate against PEL effects.

B. Optimization Strategy for Parameter Design

To balance system performance and available resources, system parameters require careful adjustment. Based on the proposed feasible parameter region, a straightforward optimization strategy for parameter design involves the following steps.

1) Initialize the upper and lower bounds of h_{RT} and O_p given the required swath width and spatial resolution, thus determining the parameter region.
2) Identify the feasible parameter region that meets the desired system performance ratios.
3) Select h_{RT} and O_p within the feasible parameter region to satisfy specific mission requirements, for example, minimizing antenna size.
4) Verify whether the available bandwidth meets condition (16) given the obtained h_{RT} and the desired range resolution; if it does not, repeat the first three steps.

The above problem can be addressed using appropriate optimization algorithms or tools.

V. Discussion

Two points warrant discussion. First, although the results use an exemplary system design, definitions of system performance ratios, related derivations, and boundary conditions are independent of any specific parameter. Thus, conclusions could be generalized to typical spaceborne SAR designs when mission requirements, azimuth parameters, antenna size, available bandwidth, and average power are similar for both F-SCAN and DBF techniques. Second, azimuth parameters affect performance ratios; however, they do not alter the conclusions and can inform parameter optimization. Future work could further investigate the joint impact of 2-D parameters on system performance.

VI. Conclusion

This letter introduces four performance ratios and presents a detailed comparative analysis of F-SCAN and DBF SAR performance. An optimization strategy is proposed by refining the feasible parameter region, providing guidelines for selecting imaging modes and tuning system parameters. The analysis indicates that F-SCAN should not be regarded as a direct replacement for DBF, as it may degrade performance in specific scenarios. Nevertheless, with sufficient available bandwidth, F-SCAN is suitable for applications requiring very wide swaths with medium- to low-range resolution.

References

[1] C. Roemer, R. Gierlich, J. Marquez-Martinez, and M. Notter, "Frequency scanning applied to wide area SAR imaging," in *Proc. EUSAR*, Jun. 2018, pp. 1–5.
[2] L. Nan, G. Gai, T. Shiyang, and Z. Linrang, "Signal modeling and analysis for elevation frequency scanning HRWS SAR," *IEEE Trans. Geosci. Remote Sens.*, vol. 58, no. 9, pp. 6434–6450, Sep. 2020.
[3] P. Guccione, D. Mapelli, D. Giudici, and A. R. Persico, "Design of f-SCAN acquisition mode for synthetic aperture radar," *Remote Sens.*, vol. 14, no. 20, p. 5283, Oct. 2022. [Online]. Available: https://www.mdpi.com/2072-4292/14/20/5283
[4] M. Younis, F. Q. de Almeida, T. Bollian, M. Villano, G. Krieger, and A. Moreira, "A synthetic aperture radar imaging mode utilizing frequency scan for time-of-echo compression," *IEEE Trans. Geosci. Remote Sens.*, vol. 60, 2022, Art. no. 5239917.
[5] B. Li, D. Liang, Y. Nan, J. Li, P. Lu, and R. Wang, "A novel nonlinear frequency scanning SAR imaging mode," *IEEE Trans. Geosci. Remote Sens.*, vol. 62, 2024, Art. no. 5220424.
[6] N. Gollin, R. Scheiber, M. Martone, P. Rizzoli, and G. Krieger, "SAR imaging in frequency scan mode: System optimization and potentials for data volume reduction," *IEEE Trans. Geosci. Remote Sens.*, vol. 61, 2023, Art. no. 5200420.
[7] Y. Zhang et al., "First demonstration of echo separation for orthogonal waveform encoding MIMO-SAR based on airborne experiments," *IEEE Trans. Geosci. Remote Sens.*, vol. 60, 2022, Art. no. 5225016.
[8] M. Younis, F. Q. de Almeida, M. Villano, S. Huber, G. Krieger, and A. Moreira, "Digital beamforming for spaceborne reflector-based synthetic aperture radar, part 1: Basic imaging modes," *IEEE Geosci. Remote Sens. Mag.*, vol. 9, no. 3, pp. 8–25, Sep. 2021.
[9] R. Song, W. Wang, Y. Zhang, Y. Wu, and W. Yu, "Improved linear PRI design strategy for HRWS continuous spaceborne SAR imaging," *IEEE Geosci. Remote Sens. Lett.*, vol. 21, pp. 1–5, 2024.